Tight focusing of radially polarized beams by a devil's vortex lens

ZIYANG CHEN, XIANSHENG HU, XUDONG CHEN, XIAOYAN WANG, JIXIONG PU[*]

Fujian Provincial Key Laboratory of Light Propagation and Transformation,
College of Information Science and Engineering, Huaqiao University,
Xiamen, Fujian361021, China

[*]Corresponding author: jixiong @hqu.edu.cn

Tight focusing of radially polarized beams with a devil's vortex lens is numerically investigated. Multiple focal spots can be generated in the geometric focus when a radially polarized beam is focused by a high numerical aperture objective in the presence of a devil's vortex lens. The position of the major focal spot shifts from the geometric focus when a devil's vortex lens with $S = 1$ is employed, and the position of the focal spot can be controlled by the numerical aperture of the objective. The intensity components of the major focal spot are influenced by the vortex phase of the devil's vortex lens. A strong longitudinal component near the optical axis is produced by a devil's vortex lens without vortex phase, and a nearly pure transversal field is produced by a devil's vortex lens with vortex phase.

Keywords: devil's vortex lens, radially polarized beam, tight focusing, high numerical aperture.

1. Introduction

A new type of diffractive optical element (DOE), namely devil's lens (DL), was introduced in 2007 [1]. A DL is a rotationally symmetric diffractive lens whose phase profile is designed from a devil's staircase function. The triadic Cantor set is often chosen as the devil's staircase function to generate DLs [2]. A single major focus and a number of subsidiary focal points are generated along the optical axis under the illumination of monochromatic irradiances. The relative intensity of the subsidiary focus of DL is stronger than that of the associated Fresnel kinoform lens [1]. Generalized devil's lenses (GDLs), whose structure is based on the generalized Cantor set, have been developed based on the concept of DL [3]. The number of subsidiary foci of a GDL is higher than that of conventional DL, and the structure of these subsidiary foci shows self-similar profile. A new kind of vortex lens, referred to as devil's vortex lens (DVL), is proposed by modulating a DL with a helical phase structure [4]. Under monochromatic illumination, a DVL produces a focal volume containing a delimited chain of vortices, which

are axially distributed according to the self-similarity of the lens. A DVL can be experimentally realized by using a spatial light modulator (SLM) [5]. Optical vortices with desired position and topological charge can be obtained by implementing arrays of DVLs in a reconfigurable SLM [6, 7]. A multilevel phase version of a DL has been reported recently [8].

Radially polarized beams focused by a high numerical aperture (high-NA) objective have been increasingly studied. It has been shown that tight focusing of radially polarized beams can have some advantages over linearly polarized beams like smaller focal spot and stronger longitudinal component. D<small>ORN</small> *et al*. demonstrated that a radially polarized field can be focused to a spot that is significantly smaller than a linearly polarized beam [9]. In addition, a stronger longitudinal electric field component can be generated under the radially polarized irradiance [10]. Interesting phenomena are observed by introducing DOEs into the high-NA focusing system. A non-diffracting and "pure" longitudinal light beam with subdiffraction beam size is created by focusing a radially polarized Bessel–Gaussian (BG) beam with a combination of a binary-phase optical element and a high-NA lens [11]. An on-axis spherical spot with controllable position is generated in a high-NA focusing system using a radially polarized beam focusing with phase modulation, which can be realized by a proper DOE [12]. B<small>OKOR</small> and D<small>AVIDSON</small> employed a radial polarization mode to create a nearly spherical central spot in the focal region, with extremely low sidelobe intensities [13]. W<small>EIBIN</small> C<small>HEN</small> and Q<small>IWEN</small> Z<small>HAN</small> generated a spherical spot by focusing a radial polarization beam with spatial amplitude modulation, and two spherical spots with diffraction-limited size and variable distance with spatial phase modulation [14].

In the present study, the tight focusing properties of radially polarized beam focused by a high-NA objective combined with DVL are investigated. The concept of DVL is introduced, and the influence of DVL on the intensity distribution near focus is analyzed.

2. Theoretical analysis

The phase distribution of a DL is characterized by the devil's staircase function. A standard example of a devil's staircase is the Cantor function, which is defined in the domain [0, 1] as [1, 2]

$$F_S(x) = \begin{cases} \dfrac{l}{2^S} & \text{if} \quad p_{S,l} \leq x \leq q_{S,l} \\[2mm] \dfrac{1}{2^S} \dfrac{x - q_{S,l}}{p_{S,l+1} - q_{S,l}} + \dfrac{l}{2^S} & \text{if} \quad q_{S,l} \leq x \leq p_{S,l+1} \end{cases} \tag{1}$$

where S is the function order, and l is the number of horizontal sections. The function has and takes on integer values from 0 to $2^S - 1$. The values of q and p are the start

and end points for each segment of the Cantor set, as described in [2], and $F_S(0) = 0$ and $F_S(1) = 1$.

From a particular Cantor function $F_S(x)$, a DL is defined as a circularly symmetric pure-phase DOE whose transmittance is defined by

$$Q(\zeta) = \exp\left[-i2^{S+1}\pi F_S(\zeta)\right] \tag{2}$$

where $\zeta = (\sin(\theta)/\sin(\alpha))^2$ is the normalized quadratic radial variable, θ is the angle of convergence, and α is the maximal convergence angle determined by the NA of the objective.

A DVL can be constructed from a conventional DL by adding a spiral phase of $\exp(im\varphi)$, where m is a non-zero integer called the topological charge and φ is the azimuthal angle. The transmittance of a DVL can be expressed as

$$T_{\mathrm{DVL}}(\theta, \varphi) = \exp\left[-i2^{S+1}\pi F_S(\theta)\right]\exp(im\varphi) \tag{3}$$

Figure 1 illustrates some examples of the phases of DVLs. The phase of a DL can be decomposed into two parts: without phase-modulated section (color in black) and with phase-modulated section (other colors), as shown in Figs. 1**a** and 1**c**. The phase of a DVL is more complicated, an additional phase change in azimuthal direction that has been determined by vortex phase is imposed.
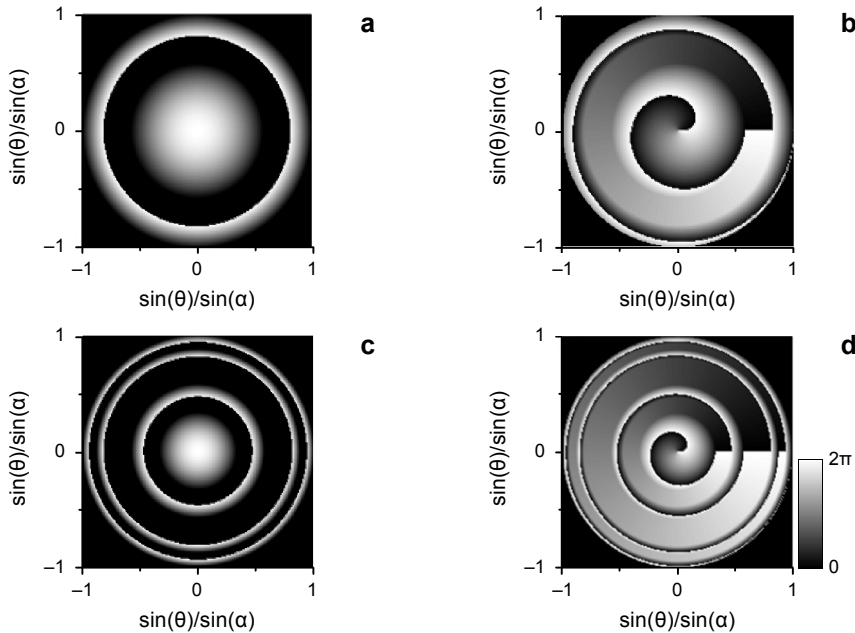

Fig. 1. Phase of DVLs: $S = 1$, $m = 0$ (**a**), $S = 1$, $m = 1$ (**b**), $S = 2$, $m = 0$ (**c**), and $S = 2$, $m = 1$ (**d**).

According to a previous study, the Cartesian components of the electric vector of radially polarized beam near focus of the high-NA objective can be described as [15]

$$
\begin{bmatrix} E_x(r, \phi, z) \\ E_y(r, \phi, z) \\ E_z(r, \phi, z) \end{bmatrix} = \frac{-i}{\pi} \int_0^\alpha \int_0^{2\pi} \sin(\theta)\sqrt{\cos(\theta)}\, P(\theta) T_{\mathrm{DVL}}(\theta, \varphi)
$$

$$
\times \exp\left\{ ik\left[z\cos(\theta) + r\sin(\theta)\cos(\varphi - \phi) \right] \right\} \begin{bmatrix} \cos(\theta)\cos(\varphi) \\ \cos(\theta)\sin(\varphi) \\ \sin(\theta) \end{bmatrix} \mathrm{d}\varphi\,\mathrm{d}\theta
$$

$$(4)$$

where θ is the angle of convergence, $T(\theta, \varphi)$ is the transmission function of the DVL, $P(\theta)$ is the pupil apodization function at the exit pupil, λ is the wavelength of the incident beam, $k = 2\pi/\lambda$ is the wave number, and $\alpha = \sin^{-1}(\mathrm{NA})$ is the maximal angle determined by the NA of the objective. Variables r, ϕ, and z are the cylindrical coordinates of an observation point near the focus.

The radial and azimuthal components of the electric vector can be obtained through the following transformations

$$E_r(r, \phi, z) = E_x(r, \phi, z)\cos(\phi) + E_y(r, \phi, z)\sin(\phi) \tag{5a}$$

$$E_\phi(r, \phi, z) = E_y(r, \phi, z)\cos(\phi) - E_x(r, \phi, z)\sin(\phi) \tag{5b}$$

As widely used in similar studies [15], we take a BG beam as an example to investigate the focusing property of a radially polarized beam focused by a high-NA objective combined with a DVL. The pupil apodization function of a BG beam can be expressed as

$$
P(\theta) = A\exp\left[-\beta_0^2\left(\frac{\sin(\theta)}{\sin(\alpha)} \right)^2 \right] J_1\left(2\beta_0 \frac{\sin(\theta)}{\sin(\alpha)} \right) \tag{6}
$$

where β_0 is the ratio of the pupil radius and the beam waist, and $J_1(x)$ is the first-order Bessel function of the first kind.

The intensities near focus can be numerically simulated by solving the resulting integral (4). In the following numerical calculations, the parameters are set as: $\beta_0 = 1.5$, $\lambda = 633$ nm, and NA = 0.9.

3. Numerical simulations

A DVL without vortex phase reduces to a conventional DL, which can be obtained by letting $m = 0$ in Eq. (3). Figure 2 shows the intensity distribution of a radially polarized beam focused by a high-NA objective combined with a DL. Only a focal spot located
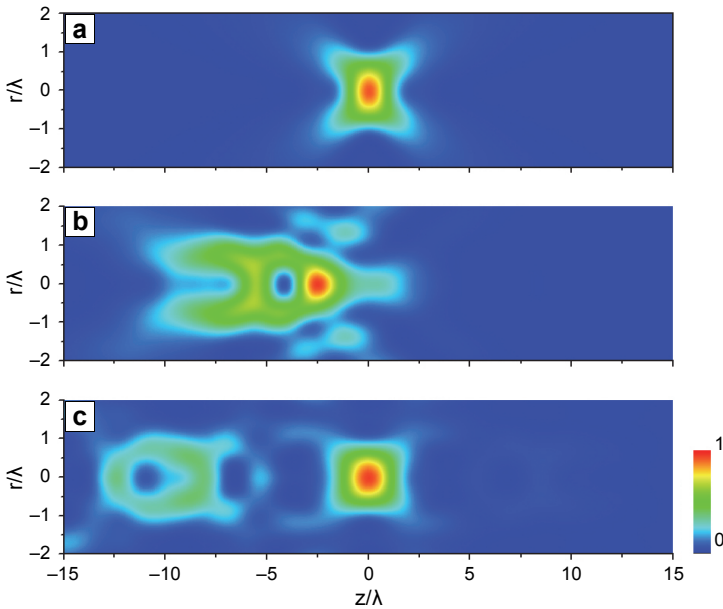
Fig. 2. Intensity of a radially polarized beam focused by a high-NA objective with a DVL of $m = 0$; $S = 0$ (**a**), $S = 1$ (**b**), and $S = 2$ (**c**).

in the geometric focus is formed with $S = 0$. It is noticed that no additional phase modulation is introduced with $S = 0$. Therefore, the result is consistent with that in [15]. Two features in Fig. 2 are notable. First, two focal spots along the axis are generated in Fig. 2**b**, but none of them are located in the geometric focus. A dark core is generated between these two focal spots. Second, a major focal spot, which is located in the geometry, and a number of subsidiary focal spots are generated with $S = 2$. The results show the influence of a DL on the intensity distribution near the focus; the position of the major focal spot is shifted with $S = 1$, and subsidiary focal spots are observed. When a radially polarized illumination without phase modulation is focused by an objective, the wavefront converges into a spherical shape and the position of the maximal intensity is the focal point. In this study, a new type of DOE (*i.e.*, DVL) is introduced. The wavefront of the illumination is modulated by a DVL. The wavefront of a beam after the DVL can be divided into two parts: with and without phase modulation, as shown in Fig. 1. For DVL with $S = 1$, the phase modulation part is dominant. The additional phase modulation influences the position of the maximal intensity location. For DVL with $S = 2$, the part without phase modulation is dominant, and the position of major focal point is the geometric focus; other subordinary focal points, which correspond to the phase modulation part, are generated as well.

Different from paraxial approximation, a longitudinal component is produced when a beam is focused by a high-NA objective. Previous study shows that longitudinal component under the illumination of radially polarized beam can be stronger than that under a linearly polarized beam [9–11]. Figure 2**b** shows that the position of the focal
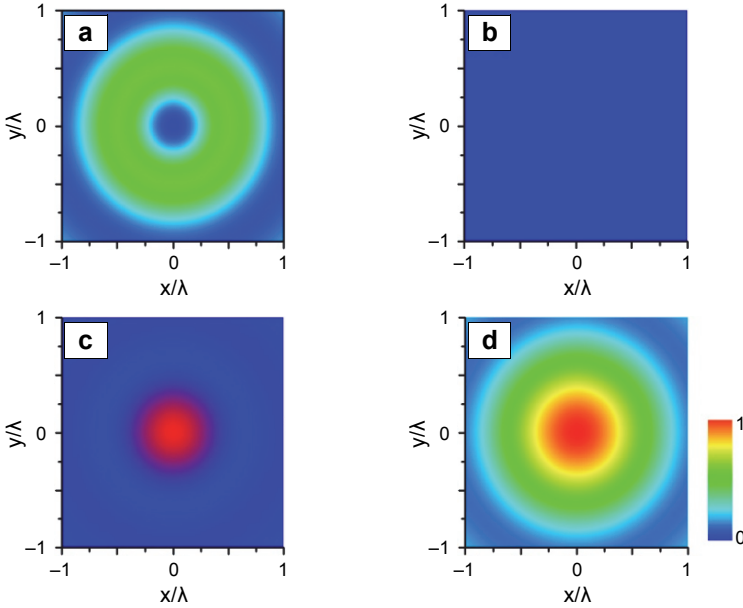
Fig. 3. Intensity of radially polarized beam focused by a high-NA objective and a DVL with $S = 1$ and $m = 0$; the other parameter is chosen as $z = -2.55\lambda$; radial component (**a**), azimuthal component (**b**), longitudinal component (**c**), and total intensity (**d**).

spot is $z = -2.55\lambda$; we take this focal spot as an example to study the components of intensity, as shown in Fig. 3. A typical radially polarized beam has a central dark core owing to the polarization singularity. However, the center of a focal spot of a radially polarized beam formed by a high-NA objective is filled with light because a strong longitudinal component is produced. The azimuthal component of the intensity is zero because of the symmetry.
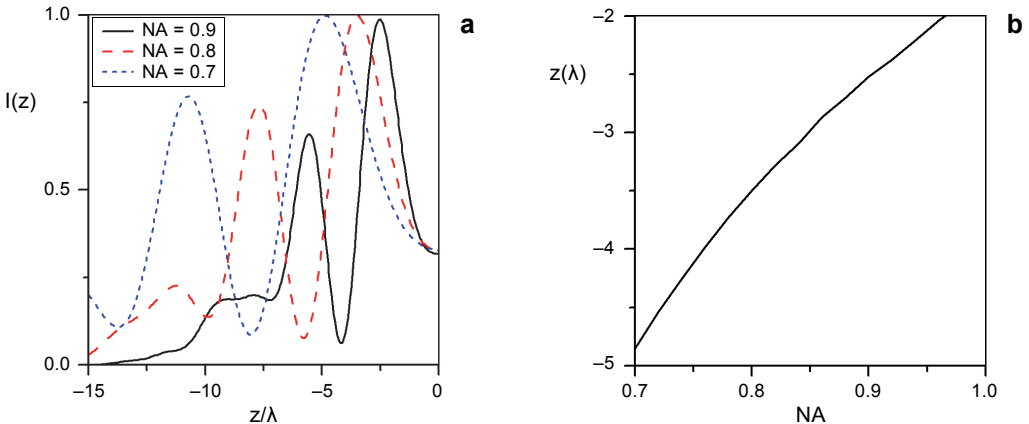

Fig. 4. On-axial intensity of radially polarized beam formed by a high-NA objective and a DVL with $S = 1$, $m = 0$ (**a**). Position of the major focal spot with different NA (**b**).
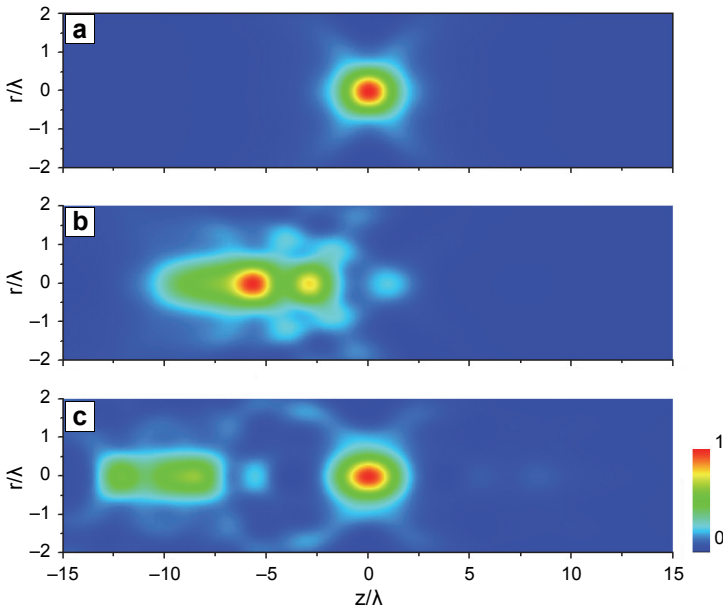
Fig. 5. Intensity of radially polarized beam focused by a high-NA objective and a DVL with $m = 1$; $S = 0$ (**a**), $S = 1$ (**b**), and $S = 2$ (**c**).

In some applications, it would be helpful if the position of the focal spot along the optical axis can be modulated. In this study, the position of the major focal spot shifts from the geometric focus when a DVL with $S = 1$ is employed. The shift of the focal spot can be explained by the influence of the additional phase modulation introduced by DVL. The on-axial intensity of the radially polarized beam formed by an objective with different NA is presented in Fig. 4**a**. The position of the focal spot varies with NA. The dependence of the position of the focal spot on the NA of the objective is plotted in Fig. 4**b**. In general, the shift of the focal spot is larger with a lower NA.

The intensity of the radially polarized beam focused by a high-NA objective combined with a DVL of $m = 1$ is presented in Fig. 5. Compared with the result in Fig. 2, some similarities are observed, such as the focal shift with a DVL of $S = 1$ and multiple focal spot with a DVL of $m = 2$. Also some differences are observed, the focal spot is smaller, and the dark core in Fig. 2**b** disappears. The intensity distribution of an ordinary radially polarized beam is a dark hollow shape because of the polarization singularity. However, a bright spot exists in the focus when a radially polarized beam focused by a high-NA objective and a DVL with $m = 1$. This can be explained by the relation of polarization and phase, *i.e.*, a change in the phase of the incident beam would result in a change in polarization.

Figure 6 shows the intensity components of the focal spot at $z = -5.66\lambda$ formed by a DVL with $m = 1$ and $S = 1$. The result is quite different from that in Fig. 3. The azimuthal intensity component is produced because of the asymmetry of the field, which arises from the azimuthal dependence of vortex phase. The field is a pure transversal
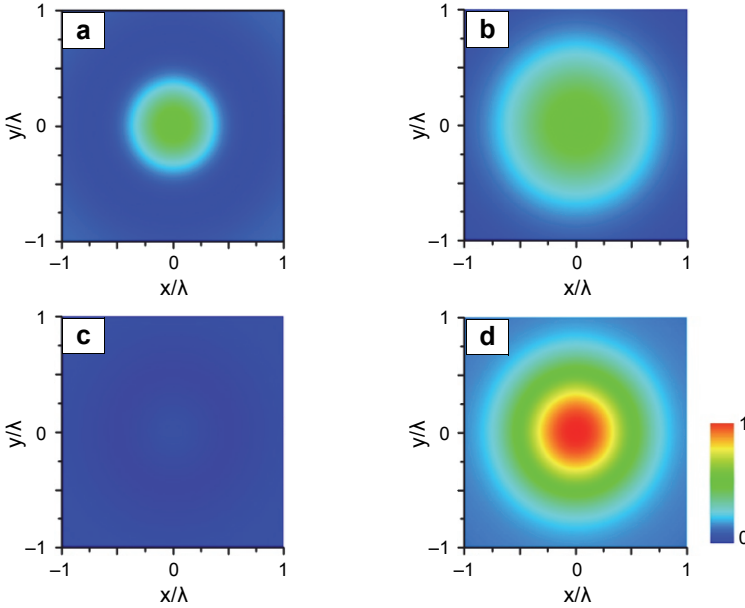
Fig. 6. Intensity of radially polarized beam focused by a high-NA objective and a DVL with $S = 1$ and $m = 1$. The other parameter is chosen as $z = -5.66\lambda$; radial component (**a**), azimuthal component (**b**), longitudinal component (**c**), and total intensity (**d**).

field because the longitudinal component is almost zero because of the destructive interference.

The intensity profile in the axis of the radially polarized formed by a high-NA objective combined with a DVL with $S = 1$ and $m = 1$ is shown in Fig. 7. Two focal spots
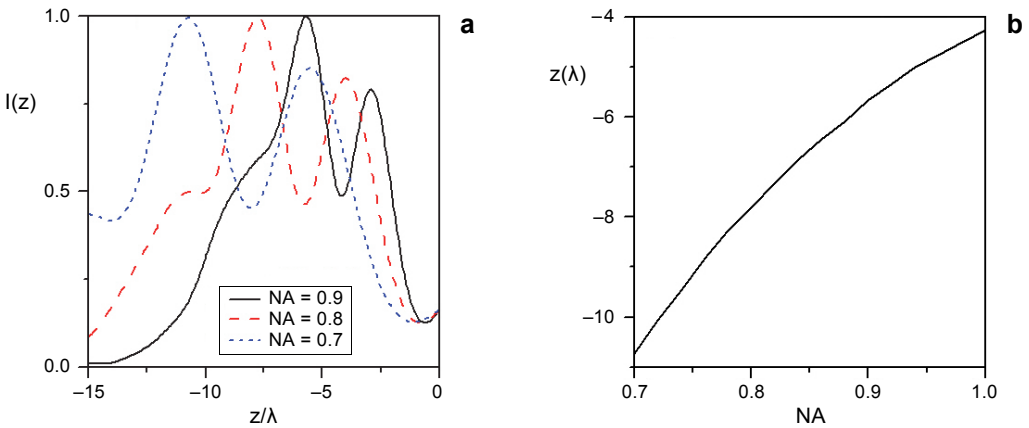

Fig. 7. On-axial intensity of radially polarized beam formed by a high-NA objective and a DVL with $S = 1$, $m = 1$ (**a**). Position of the major focal spot with different NA (**b**).

are generated in the axis, and the positions of these spots depend on the NA of the objective, as shown in Fig. 7**b**. The distance between the focal spot and the geometric focus can be larger than 10λ, and the magnitude decreases with increasing NA.

4. Conclusion

We have studied the intensity near focus of a radially polarized beam focused by a high -NA objective combined with a DVL. The results showed that the intensity of the beam with a DVL is different from that without a DVL. The intensity depends on the structure of the DVL. Only a focal spot located in the geometric focus can be obtained without a DVL. However, multiple focal spots can be generated in the presence of a DVL. The position of the major focal spot shifted from the geometric focus when a DVL with $S = 1$ is employed, and the position of the focal spot can be controlled by the NA of the objective. The intensity components of the major focal spot with different vortex phases were studied by using a DVL with $S = 1$. Results showed that a strong longitudinal component near the optical axis is produced by a DVL without vortex phase, and a nearly pure transversal field is produced by a DVL with $m = 1$. These results may have potential applications in particle trapping. We have demonstrated an optical tweezers using a laser beam on which is imprinted a focusing phase profile generated by a DVL [16]. A variety of micron and submicron-sized particles can be trapped by beam shaped with DVL, and the optical trap strength is influenced by the structure of a DVL. The difference between this study and our previous study is that radially polarized beam is used as illumination, so a stronger longitudinal component can be achieved. A strong longitudinal field has many attractive applications, for example, in particle trapping [17], fluorescent imaging [18].

References

[1] MONSORIU J.A., FURLAN W.D., SAAVEDRA G., GIMÉNEZ F., *Devil's lenses*, Optics Express 15(21), 2007, pp. 13858–13864.

[2] CHALICE D.R., *A characterization of the Cantor function*, The American Mathematical Monthly 98(3), 1991, pp. 255–258.

[3] CASANOVA C., FURLAN W.D., REMÓN L., CALATAYUD A., MONSORIU J.A., MENDOZA-YERO O., *Self-similar focusing with generalized devil's lenses*, Journal of the Optical Society of America A 28(2), 2011, pp. 210–213.

[4] FURLAN W.D., GIMÉNEZ F., CALATAYUD A., MONSORIU J.A., *Devil's vortex-lenses*, Optics Express 17(24), 2009, pp. 21891–21896.

[5] MITRY M., DOUGHTY D.C., CHALOUPKA J.L., ANDERSON M.E., *Experimental realization of the devil's vortex Fresnel lens with a programmable spatial light modulator*, Applied Optics 51(18), 2012, pp. 4103–4108.

[6] Calabuig A., Sánchez-Ruiz S., Martínez-León L., Tajahuerce E., Fernández-Alonso M., Furlan W.D., Monsoriu J.A., Pons-Martí A., *Generation of programmable 3D optical vortex structures through devil's vortex-lens arrays*, Applied Optics 52(23), 2013, pp. 5822–5829.

[7] Calatayud A., Rodrigo J.A., Remón L., Furlan W.D., Cristóbal G., Monsoriu J.A., *Experimental generation and characterization of devil's vortex-lenses*, Applied Physics B 106(4), 2012, pp. 915–919.

[8] Dong Wu, Li-Gang Niu, Qi-Dai Chen, Rui Wang, Hong-Bo Sun, *High efficiency multilevel phase-type fractal zone plates*, Optics Letters 33(24), 2008, pp. 2913–2915.

[9] Dorn R., Quabis S., Leuchs G., *Sharper focus for a radially polarized light beam*, Physical Review Letters 91(23), 2003, article ID 233901.

[10] Urbach H.P., Pereira S.F., *Field in focus with a maximum longitudinal electric component*, Physical Review Letters 100(12), 2008, article ID 123904.

[11] Haifeng Wang, Luping Shi, Lukyanchuk B., Sheppard C., Chong Tow Chong, *Creation of a needle of longitudinally polarized light in vacuum using binary optics*, Nature Photonics 2, 2008, pp. 501–505.

[12] Shaohui Yan, Baoli Yao, Rupp R., *Shifting the spherical focus of a 4Pi focusing system*, Optics Express 19(2), 2011, pp. 673–678.

[13] Bokor N., Davidson N., *Toward a spherical spot distribution with 4π focusing of radially polarized light*, Optics Letters 29(17), 2004, pp. 1968–1970.

[14] Weibin Chen, Qiwen Zhan, *Creating a spherical focal spot with spatially modulated radial polarization in 4Pi microscopy*, Optics Letters 34(16), 2009, pp. 2444–2446.

[15] Youngworth K.S., Brown T.G., *Focusing of high numerical aperture cylindrical-vector beams*, Optics Express 7(2), 2000, pp. 77–87.

[16] Jixiong Pu, Jones P.H., *Devil's lens optical tweezers*, Optics Express 23(7), 2015, pp. 8190–8199.

[17] Qiwen Zhan, *Trapping metallic Rayleigh particles with radial polarization*, Optics Express 12(15), 2004, pp. 3377–3382.

[18] Novotny L., Beversluis M.R., Youngworth K.S., Brown T.G., *Longitudinal field modes probed by single molecules*, Physical Review Letters 86(21), 2001, pp. 5251–5254.